mon soil suites, mare and highland, known to exist on the moon.

One important aspect of this x-ray frequency distribution is that the chemistry of returned samples may be placed in the context of the broader orbital coverage of the lunar surface. The ranges of Al/Si concentration ratios based on chemical analyses of soils from all Apollo and Luna missions are indicated by horizontal bars in Fig. 2. The frequency of occurrence for the soil ranges shown indicates the degree to which that material is representative of the areas overflown by the Apollo spacecrafts.

It is of interest to note that within the quality of the measurements there appear to be compositional continua about both highland and mare modes. There does not appear to be any significant amount of material within the mapped area having Al/Si values lower than those of the Apollo 17 black and orange soils.

The following geochemical features seen on the image are useful clues to lunar evolutionary processes.

1) The chemical composition of the maria becomes more aluminous from west to east.

2) Nonmare areas become increasingly Al-rich from west to east, with the exception of the Descartes area (17°E; 8°S), which has Al/Si values as high as those of highland areas east of 40°E.

3) Considerable variation in Al/Si values within highland areas demonstrates that the lunar crust is not homogeneous.

4) It is apparent from variations in Al/Si that the Smythii basin (80°E to 90°E; 5°S to 5°N) is only partially flooded with basalt.

5) A concentric pattern of Al/Si variations around the Crisium basin (50°E to 65°E; 10°N to 20°N) suggests a chemical correlation with the topographic expression of a multiple ring system. This pattern may represent disruption of crustal stratigraphy or mare basalt flooding in the topographic lows between the rings. A more detailed analysis is required to resolve this question.

6) Low Al/Si values immediately to the west of and within the Firmicus crater (63°E; 8°N) and within the Miraldi crater (35°E; 19°N) support photogeologic evidence that mare basalts have flooded the floors of these craters. Identification of these basalt-filled highland craters, which have distinct Al/Si signatures, provides information about the volumes and distribution patterns of mare basalt flows on the lunar surface.

7) The postmare crater, Langrenus (61°E; 8°S), exhibits a traceable high-Al/Si ejecta blanket extending west into Mare Fecunditatis. This ejecta is detectable from x-ray data because the highland-type material displaced contrasts chemically with the adjacent mare surface. The extent of primary ejecta in proportion to the crater size is significant for studies of crater mechanics and for volume estimates of material excavated by meteorite impact.

8) The craters Capella (35°E; 7.5°S), Apollonius A (57°E; 5°N), and Taruntius (46.5°E; 5.5°N) have higher Al/Si values than the adjacent intermare areas, suggesting that the impacts exposed a lower stratigraphic horizon of higher Al/Si material.

9) The postmare craters Plinius (24°E; 15.5°N) and Ross (22°E; 12°N) appear to have penetrated thin mare basalts and excavated material from the more aluminous basin floor zone. The nature of subsurface material may be observed through the "window" of impact craters. The depths of craters which sample basin floor material help to define submare basin morphology and constrain estimates of the maximum depth of mare basalt flows.

10) A streak of lower Al/Si values crosses both Mare Fecunditatis and highland areas from southwest to northeast (intersecting coordinates 59°E; 3°N and 54°E; 2°S). This streak is parallel to and only slightly offset from a mapped ray radial to the Tycho event.

Finally, it is worth noting that the area mapped to date from x-ray data constitutes less than 10 percent of the lunar surface. For complete interpretation of these data and for full exploitation of the Apollo and Luna returned lunar sample information, it is of utmost importance that x-ray data be obtained over the whole moon so that the full range of surface soil compositions may be characterized and mapped in detail. The opportunity to accomplish this important goal is readily available in the projected Lunar Polar Orbiter mission, with its global mapping capability.

CONSTANCE G. ANDRE
Chemistry Department, University of Maryland, College Park 20742
MICHAEL J. BIELEFELD
Computer Sciences Corporation, Silver Spring, Maryland 20910
ERIC ELIASON
LAURENCE A. SODERBLOM
U.S. Geological Survey, Flagstaff, Arizona 86001
ISIDORE ADLER
Chemistry Department, University of Maryland, College Park 20742
JOHN A. PHILPOTTS
Goddard Space Flight Center, Greenbelt, Maryland 20771

References and Notes

1. I. Adler, J. Gerard, J. Trombka, R. Schmadebeck, P. Lowman, H. Blodget, L. Yin, E. Eller, R. Lamothe, P. Gorenstein, P. Bjorkholm, B. Harris, H. Gursky, in *Proceedings of the Third Lunar Science Conference*, D. Criswell, Ed. (MIT Press, Cambridge, Mass., 1972), vol. 3, pp. 2157–2178.
2. I. Adler *et al.*, *Science* **177**, 256 (1972).
3. I. Adler, J. Trombka, R. Schmadebeck, P. Lowman, H. Blodget, L. Yin, E. Eller, M. Podwysocki, J. R. Weidner, A. L. Bickel, R. K. L. Lum, in *Proceedings of the Fourth Lunar Science Conference*, W. Gose, Ed. (Pergamon, Elmsford, N.Y., 1973), vol. 1, frontispiece.
4. M. H. Podwysocki, J. R. Weidner, C. G. Andre, A. L. Bickel, R. S. Lum, I. Adler, J. E. Trombka, in *Proceedings of the Fifth Lunar Science Conference*, W. Gose, Ed. (Pergamon, Elmsford, N.Y., 1974), vol. 3, pp. 3017–3024.
5. We gratefully acknowledge use of the imaging facilities of Code 930 of Goddard Space Flight Center. Supported by NASA grant NGR-21-002-368.

22 June 1977; revised 19 July 1977

Nucleon Stability: A Geochemical Test Independent of Decay Mode

Abstract. *By analyzing published geochemical data on xenon isotopes measured in a 2.46 × 10⁹-year-old telluride ore, a lower limit of 1.6 × 10²⁵ years has been obtained for the mean lifetime of the nucleons in the tellurium-130 nucleus. This result is insensitive to the particular mode by which the nucleons decay and therefore provides a rigorous limit on possible baryon number nonconservation. The new limit is about two orders of magnitude better than the previous rigorous limit on nucleon stability.*

The law of baryon conservation, first proposed by Stückelberg (*1*) and by Wigner (*2*), has recently received renewed attention because of the prediction by several unified gauge theories (*3*) of the weak, electromagnetic, and strong interactions that this law may not be exact (*4*). From an experimental point of view, the most sensitive tests of baryon conservation are provided by searches for decays of nucleons (*5*), since such decays, at least into known particles, cannot occur without violating the law of baryon conservation. Estimates of the nucleon lifetime provided by the various unified gauge theories (*3*) range from 10^{27} to 10^{35} years.

A limit of 2×10^{30} years has been placed on the nucleon lifetime by Reines and Crouch (*6*), using data from an underground neutrino experiment. This experiment, however, was sensitive only to decay modes in which an energetic muon or pion is produced. Positron-emitting modes such as $p \rightarrow e^+ + \gamma$ and neutral modes such as $n \rightarrow 3\nu$ or $p \rightarrow 3\nu$ (*7, 8*), for example, are not accessible by this method. It is therefore desirable to set rigorous limits for nucleon stability by using techniques that are insensitive to the decay mode. At present, the best rigorous limit on nucleon stability, 2×10^{23} years, was obtained in an experiment (*9*) searching for the spontaneous fission of ^{232}Th after excitation by nucleon decay. The present best rigorous limit on proton stability, 3×10^{23} years, was set in an experiment (*10*) sensitive to the neutron left behind by decay of the proton in deuterium.

Rosen (*11*) has discussed the possibility of using geochemical techniques to search for nucleon decay. Such techniques would have the advantage of integrating over large time spans. The possibility of searching for rare gas anomalies in ancient ores containing ^{23}Na, ^{39}K, $^{85-87}$Rb, and ^{133}Cs was considered. None of these cases, however, appeared to be very favorable for greatly extending the existing nucleon lifetime limit.

We have found that a significant improvement in this limit can be obtained by the study of xenon isotope anomalies in ores containing ^{130}Te. Careful measurements of the xenon isotopes in a variety of dated tellurium ores have already been completed in experiments (*12, 13*) investigating the double beta-decay of ^{130}Te and ^{128}Te. Strong evidence for the existence of the double beta-decay process has been obtained by these methods, and good estimates of double beta-decay lifetimes have been published.

The new nucleon stability limit can be estimated from this work by the following considerations. The disappearance of a nucleon from ^{130}Te would produce either ^{129}Te (for neutron decay) or ^{129}Sb (for proton decay). In general, the mass 129 nucleus would be formed in an excited state, whose excitation energy, E_{ex}, is approximated by

$$E_{ex} = E_b - E_s$$

where E_b is the binding energy of the decaying nucleon and E_s is the binding energy of the least bound nucleon in ^{130}Te. Thus, for protons

$$E_{ex} = E_b - 10.0 \text{ Mev}$$

and for neutrons

$$E_{ex} = E_b - 8.4 \text{ Mev}$$

Table 1. Reduced xenon data of Hennecke *et al.* (*13*) (600°C temperature fraction). Values are volume at standard temperature and pressure (STP) per gram.

Isotope	Xenon content ($\times 10^{-13}$ cm^3 STP g^{-1})		
	Total	Atmospheric component	Net excess
Xenon-128	0.63	0.34	0.29
Xenon-129	11.0	4.63	6.37
Xenon-130	509.7	0.72	509.0
Xenon-131	6.27	3.71	2.56
Xenon-132	4.71	4.71	

If E_{ex} is less than the binding energy of the least bound nucleon in the mass 129 daughter nucleus, energy conservation requires that nucleus to de-excite by gamma emission rather than by nucleon emission (*14*). Therefore, for proton decay, we require

$$E_b \leqq 10.0 + 8.0 = 18.0 \text{ Mev} \quad (1)$$

and for neutron decay

$$E_b \leqq 8.4 + 6.1 = 14.5 \text{ Mev} \quad (2)$$

If these inequalities are satisfied, nucleon decay in ^{130}Te will produce a mass 129 nucleus with 100 percent probability. If the inequalities are not satisfied, nucleon decay in ^{130}Te will be followed by particle emission from the mass 129 daughter nucleus. We must therefore determine the number of nucleons in ^{130}Te that have binding energies less than 18.0 Mev (for protons) and less than 14.5 Mev (for neutrons). A simple shell model picture of the ^{130}Te nucleus can be used for this purpose. For the neutrons, we consider the core to consist of 50 neutrons. The remaining 28 neutrons occupy, successively, the $1g_{7/2}$, $2d_{5/2}$, $1h_{11/2}$, and $2d_{3/2}$ orbits. The neutron binding energies for these orbits, allowing 1 Mev for pairing effects, are about 8 Mev (*15*). It is clear that all 28 of these neutrons satisfy inequality 2 and are therefore suitable candidates for the nucleon stability test.

Similar arguments can be made for the 52 protons. We consider them to be arranged in a core of 50 protons plus two valence protons. The outermost shells in the core consist of the 30 protons of the $1f_{7/2}$, $2p_{3/2}$, $1f_{5/2}$, $2p_{1/2}$, and $1g_{9/2}$ orbits. The binding energies of these protons have their centroid at approximately 12 Mev with a full width at half maximum of about 10 Mev (*16*). We therefore conservatively estimate that three-quarters of them have a binding energy that satisfies inequality 1. Including the two valence protons, we conclude that the effective number of protons is 24. We have, therefore, $28 + 24 = 52$ nucleons in all contributing to the nucleon decay signal.

The possibility that one of the nucleon decay products is a pion must be considered, since this would add additional excitation energy and thus reduce sensitivity by removing the product from the mass 129 isobar in some fraction of decays. Reines and Crouch (*6*) have already placed a much more stringent limit on this decay mode for charged pions, which thus can be ignored. In the case of neutral decay, sensitivity would be somewhat reduced if a neutral pion were one of the decay products. The magnitude of the effect is difficult to estimate and will be ignored in our calculations.

After several successive β^- decays, the mass 129 daughter nuclei ultimately produce ^{129}Xe, the only member of the mass 129 isobar that does not undergo beta-decay. The mean lifetime of the nucleon is therefore determined simply as the product of the mean lifetime of ^{130}Te for double beta-decay, the effective number of nucleons per nucleus (52), and the ^{130}Xe/^{129}Xe ratio after corrections for other sources of xenon have been made. The best measurement of ^{130}Xe produced by double beta-decay appears to be that of Hennecke *et al.* (*13*) on a $(2.46 \pm 0.08) \times 10^9$-year-old sample of telluride ore from Kalgoorlie, Australia. In addition to having a large amount of excess ^{130}Xe, this sample is rather low in cosmic ray–produced ^{129}Xe and ^{131}Xe. The mean lifetime of ^{130}Te for double beta-decay obtained in this work was 1.4×10^{21} years (*17*).

Using ^{132}Xe to measure atmospheric contamination, we calculated the excess amounts of xenon released in the 600°C temperature fraction as given in Table 1. By attributing all of the excess ^{129}Xe to nucleon decay, a conservative lower limit of 5.8×10^{24} years is obtained for the mean nucleon lifetime. A somewhat better limit can be deduced by correcting for cosmic-ray production of ^{129}Xe. Takagi *et al.* (*18*) have discussed the processes leading to production of ^{129}Xe and ^{131}Xe from muon interactions underground. Xenon-131 is produced mainly by neutron capture on ^{130}Te. Production of ^{129}Xe, however, can be caused by a number of processes, including capture of stopped negative muons on ^{130}Te, photonuclear excitation of ^{130}Te by fast muons, as well as neutron capture on ^{128}Te. Takagi *et al.* measured the ratio of excess ^{129}Xe to excess ^{131}Xe in several different telluride samples and found values between 1.6 and 5.5, which generally increased with depth. The small amounts of ^{129}Xe and ^{131}Xe per year found in the Kalgoorlie telluride indicate a greater average burial depth than that of any of the samples measured by these authors. Using a ratio of 1.6 should provide a conservative value for the cosmic ray–induced ^{129}Xe component. The nucleon lifetime limit thus obtained is 1.6×10^{25} years (*19*). This is probably an underestimate since it is possible that all of the observed excess ^{129}Xe is produced by cosmic rays. The observed ratio of 2.5 seems, if anything, unexpectedly low.

The nucleon lifetime limit obtained in this work represents an improvement by about two orders of magnitude over the previous (*9*) rigorous limit on nucleon stability. Some further improvement could probably be obtained if a sample with greater average burial depth were available. Uncertainties in background effects, however, would probably prevent any very large improvement.

Alternative approaches to this problem have been described (*20, 21*) in which very large samples with favorable radiochemical properties are used to search with high sensitivity for a small number of nucleon decay–produced radioactive atoms. Such methods are capable of measuring nucleon lifetimes greater than 10^{28} years. In addition, background effects (other than those due to neutrino interactions) could be controlled through burial depth, local shielding, and sample prepurification.

JOHN C. EVANS, JR.*
Chemistry Department, Brookhaven National Laboratory, Upton, New York 11973

RICHARD I. STEINBERG
Physics Department, University of Pennsylvania, Philadelphia 19104

References and Notes

1. E. C. G. Stückelberg, *Helv. Phys. Acta* **11**, 317 (1938).
2. E. P. Wigner, *Proc. Am. Philos. Soc.* **93**, 521 (1949); *Proc. Natl. Acad. Sci. U.S.A.* **38**, 449 (1952).
3. J. C. Pati and A. Salam, *Phys. Rev. Lett.* **31**, 661 (1973); *Phys. Rev. D* **8**, 1240 (1973); *ibid.* **10**, 275 (1974); H. Georgi and S. L. Glashow, *Phys. Rev. Lett.* **32**, 438 (1974); H. Georgi, H. R. Quinn, S. Weinberg, *ibid.* **33**, 451 (1974).
4. The possibility of baryon nonconservation was discussed by G. Feinberg and M. Goldhaber [*Proc. Natl. Acad. Sci. U.S.A.* **45**, 1301 (1959)].
5. We are excluding the well-known possibility of beta-decay of free neutrons and certain bound nucleons.
6. F. Reines and M. F. Crouch, *Phys. Rev. Lett.* **32**, 493 (1974).
7. Abbreviations: p, proton; e^+, positron; γ, gamma; n, neutron; and ν, neutrino.
8. Note that the last-mentioned mode implies simultaneous violation of baryon conservation and electric charge conservation. The experimenter would be wise not to exclude such processes from consideration a priori.
9. G. N. Flerov, D. S. Klochkov, V. S. Skobkin, V. V. Terent'ev, *Sov. Phys. Dokl.* **3**, 79 (1958).
10. F. E. Dix, thesis, Case Western Reserve University (1970).
11. S. P. Rosen, *Phys. Rev. Lett.* **34**, 774 (1975).
12. T. Kirsten and H. W. Müller, *Earth Planet. Sci. Lett.* **6**, 271 (1969).
13. E. W. Hennecke, O. K. Manuel, D. D. Sabu, *Phys. Rev. C* **11**, 1378 (1975).
14. We neglect alpha-particle emission, which would be highly suppressed by Coulomb barrier effects.
15. A. Calboreanu and S. Mancas, *Nucl. Phys. A* **266**, 72 (1976).
16. G. Jacob and Th. A. J. Maris, *Rev. Mod. Phys.* **45**, 6 (1973).
17. There is some uncertainty in the literature as to the precise value of this lifetime. To be conservative, we have chosen the most recently published value, which also happens to be among the lowest. For a relatively recent summary of the literature, see H. R. Hiddleston and C. P. Browne [*Nucl. Data Sheets* **13**, 133 (1974)].
18. J. Takagi, W. Hampel, T. Kirsten, *Earth Planet. Sci. Lett.* **24**, 141 (1974).
19. The nucleon lifetime limit τ is obtained as
$$\tau = \tau_{\beta\beta} \times 52 \times \frac{^{130}\mathrm{Xe}^c}{^{129}\mathrm{Xe}^c}$$
where ^{130}Xe^c is the net ^{130}Xe produced by double beta-decay and ^{129}Xe^c is given by $^{129}\mathrm{Xe}^c = {}^{129}\mathrm{Xe}^{net} - 1.6\ ({}^{131}\mathrm{Xe}^{net})$, using values given in Table 1 and $\tau_{\beta\beta} = 1.4 \times 10^{21}$ years. It is assumed that there are 52 nucleons per nucleus available for decay.
20. R. I. Steinberg and W. Maenhaut, *Lett. Nuovo Cimento* **15**, 93 (1976).
21. R. I. Steinberg, J. C. Evans, Jr., E. L. Fireman, paper presented at the International Conference on Neutrino Physics, Elbrus, Soviet Union, June 1977.
22. We thank M. Goldhaber for helpful discussions on this subject and R. Davis, Jr., for providing encouragement as well as pointing out several key references. Research was carried out at Brookhaven National Laboratory under contract with the Energy Research and Development Administration and supported by its Division of Physical Research. Research carried out at the University of Pennsylvania was supported in part by the Energy Research and Development Administration and by the Research Corporation.
* Present address: Physical Sciences Department, Battelle-Northwest, Richland, Wash. 99352.

17 February 1977; revised 31 May 1977

Microwave Spectroscopic Imagery of the Earth

Abstract. *The microwave spectrometer on the Nimbus 6 satellite has produced the first microwave spectral images of the earth. It has yielded global maps of (i) atmospheric temperature profiles, (ii) the distributions of water vapor and liquid water over ocean, and (iii) the coverage and type of ice and snow. The method has potential for operational synoptic monitoring.*

The use of passive microwave techniques to monitor geophysical phenomena began with radio astronomical observations of the solar system and the terrestrial atmosphere and surface (*1, 2*). The general principles of passive microwave sensing have been reviewed by Staelin (*3*).

The first spacecraft instrument to combine microwave spectrometry with imaging is the scanning microwave spectrometer (SCAMS). It was launched on 12 June 1975 together with companion sensors operating at visible, infrared, and a single microwave frequency. Most of these experimental sensors, including SCAMS, were designed as precursors to systems for the operational monitoring of the earth.

One of the primary objectives of the SCAMS experiment was to carry out global observations at 12-hour intervals of three geophysical parameters: atmospheric temperature profiles between altitudes of 0 and 20 km, the distributions of precipitable atmospheric water vapor and liquid water over ocean, and the microwave spectral emission of land, snow, and ice. A second goal was to determine the accuracy with which such parameters can be measured. The third aim consisted of a scientific and engineering evaluation of SCAMS and of similar microwave-sensing systems as one element in a global system for data collection.

The SCAMS system was fabricated at the Jet Propulsion Laboratory of the California Institute of Technology. It is

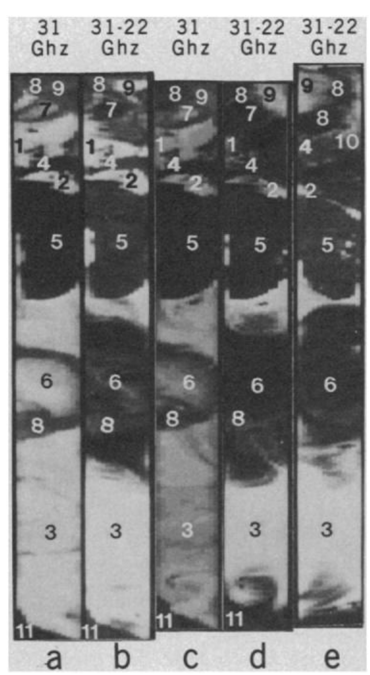

Fig. 1. Brightness temperature images for three orbits: (a and b) orbit 431, 14 July 1975; (c and d) orbit 2375, 6 December 1975; and (e) orbit 2449, 11 December 1975. In each image darker elements correspond to relatively higher brightness temperatures at 31.65 Ghz. Europe and Africa are seen in the top half of each image and Antarctica is in the center; however, in (e) the pass descended westward over Africa so as to include more of Asia than in (a) through (d). The images are compressed at the sides because the 13 view angles are equally spaced horizontally. Areas: 1, North Atlantic; 2, Mediterranean; 3, Pacific; 4, Europe; 5, Africa; 6, Antarctica; 7, Greenland; 8, newer sea ice; 9, older sea ice; 10, Siberian snow; and 11, North America.